New Journal of Physics
The open access journal at the forefront of physics

Deutsche Physikalische Gesellschaft DPG
IOP Institute of Physics

Published in partnership with: Deutsche Physikalische Gesellschaft and the Institute of Physics

OPEN ACCESS

RECEIVED
30 March 2018

REVISED
8 June 2018

ACCEPTED FOR PUBLICATION
11 June 2018

PUBLISHED
25 June 2018

PAPER

Quantum phase transitions and the degree of nonidentity in the system with two different species of vector bosons

A M Belemuk[1,2], N M Chtchelkatchev[1,2,3,7,8], A V Mikheyenkov[1,2,4] and K I Kugel[5,6]

[1] Institute for High Pressure Physics, Russian Academy of Sciences, Moscow (Troitsk) 108840, Russia
[2] Department of Theoretical Physics, Moscow Institute of Physics and Technology (State University), Moscow 141700, Russia
[3] L.D. Landau Institute for Theoretical Physics, Russian Academy of Sciences, Moscow 119334, Russia
[4] National Research Centre 'Kurchatov Institute', Moscow 123182, Russia
[5] Institute for Theoretical and Applied Electrodynamics, Russian Academy of Sciences, Moscow 125412, Russia
[6] National Research University Higher School of Economics, Moscow 101000, Russia
[7] Ural Federal University, 620002 Ekaterinburg, Russia
[8] Author to whom any correspondence should be addressed.

E-mail: nms@itp.ac.ru

Keywords: optical lattice, quantum phase transition, bosonic magnetism, strongly correlated systems, atom nonidenity

Abstract

We present new results for the system with two species of vector bosons in an optical lattice. In addition to the standard parameters characterizing such a system, we are dealing here with the 'degree of atomic nonidentity', manifesting itself in the difference of tunneling amplitudes and on-site Coulomb interactions. We obtain a cascade of quantum phase transitions occurring with the increase in the degree of atomic nonidentity. While in the system of nearly identical vector bosons only one phase transition between two phases occurs with the evolution of the interparticle interaction, atom nonidentity increases the number of possible phases to six and the resulting phase diagrams are so nontrivial that we can speculate about their evolution from the images similar to the 'J Miró-like paintings' to 'K Malewicz-like' ones.

1. Introduction

Experimental research of ultracold atoms in optical lattices have dramatically expanded the possibilities of a tunable simulation in quantum many-body physics [1–14]. Moreover, ultracold atoms open the path to the parameter range that is hardly possible or even impossible to achieve in the natural condensed matter systems [15–21].

The typical example is the system of vector bosons. This case corresponds to Bose–Hubbard model that is absent in the standard solid state theory and is the topic of intensive research last time [22–34], and [35–37] for review. Numerous striking effects, in particular, induced by the multispecie nature of boson system have been found recently including quantum phase transitions, many-body localization, and topological order, as well as the superfluidity and supersolidity of ultracold atomic systems [35–37]. Here, we focus on still unexplored physical phenomena in the systems with different species of vector bosons originating from the tunable interplay of spin degrees of freedom and of those identifying different sorts of atoms. Then the situation becomes quite intriguing: in addition to the standard parameters, there appear nontrivial ones related to the 'degree of atomic nonidentity': the difference of tunneling amplitudes and on-site interactions. We address here new physical effects including quantum phase transitions driven by atom nonidentity.

Vector cold atoms in optical lattices are characterized in general by the following parameters: intersite hopping amplitudes t_α, where $\alpha = 1, 2$ labels different atoms, on-site $U_{\alpha,\alpha'}$ Coulomb interactions, and spin channel interaction parameters U_s [31, 38].

In our recent paper [31], we have considered the simplest limiting case of nearly identical bosons in the Mott insulating state: $U_{12} \simeq U_{11} \simeq U_{22} = U_0$ and $t_1 \simeq t_2 \ll U_0$. This model differs from the case of perfectly identical bosons just by the absence of cross-tunneling term: tunneling with the change of boson identity was forbidden. It has been shown in [31] that such model can be reduced to the Kugel–Khomskii [39] type

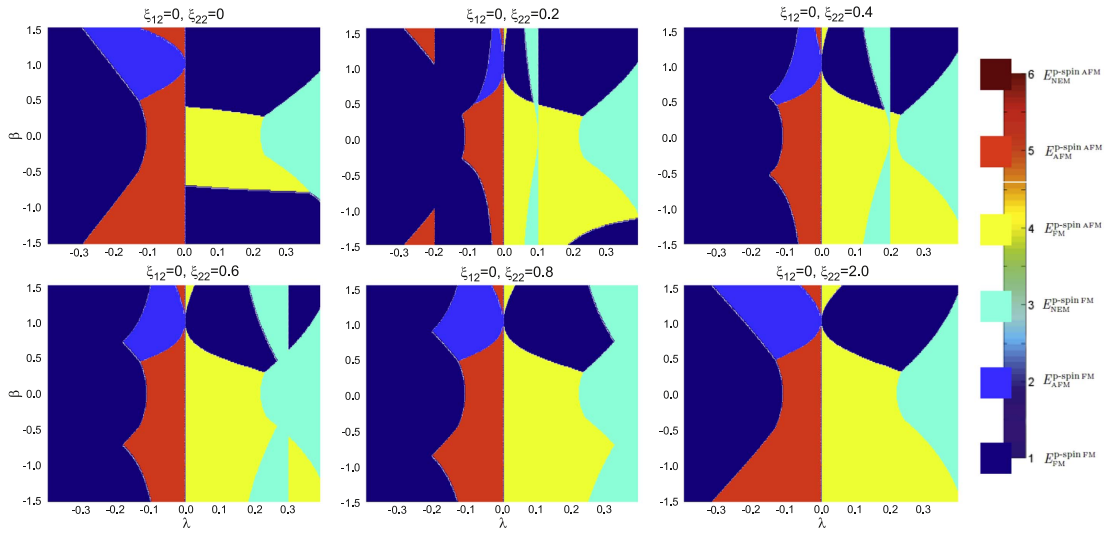

Figure 1. Phase diagrams for $\xi_{12} = U_{12}/U_{11} = 0$. Here $\beta = t_2/t_1, \xi_{22} = U_{22}/U_{11}$ and $\lambda = U_s/U_{11}$. In this case, there is no Coulomb interaction between atoms of different kinds. The colorbar defines different spin and pseudospin orders.

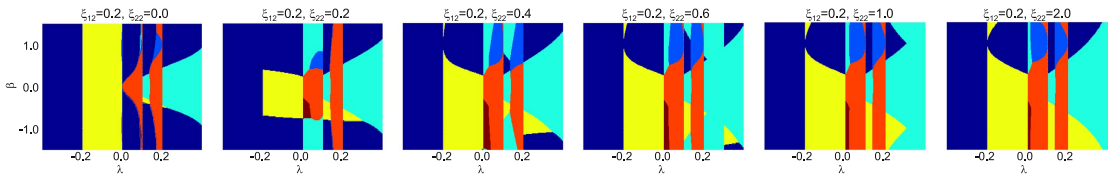

Figure 2. Phase diagrams for small Coulomb interaction between different kinds of atoms: $\xi_{12} = U_{12}/U_{11} = 0.2$. All the notations follow figure 1.

spin-pseudospin model, but in contrast to the usual version of the latter model, here spin is $S = 1$ and pseudospin-1/2 (where pseudospin labels different bosons). New effects in [31] have been found, in particular, that the ground state of the system always has the pseudospin domain structure while sign change of U_s switches the spin arrangement of the ground state within domains from ferro to aniferromagnetic (AFM).

Here we also consider two species of vector bosons in an optical lattice, but we get rid of the identity conditions $U_{12} \simeq U_{11} \simeq U_{22} = U_0, t_1 \simeq t_2$ and trace the evolution of the system quantum state with the increase in the degree of atomic nonidentity ($\beta = t_2/t_1, \xi_{12} = U_{12}/U_{11}$ and $\xi_{22} = U_{22}/U_{11}$) starting from nearly identical atoms of [31].

Surprisingly, instead of some naive and predictable modification of our previous results [31], we find that the boson system evolves between six quantum states instead of two in [31] and the manifold of quantum phase transitions is so nontrivial that one can even compare the resulting phase diagrams with modern art paintings (we find some similarity with 'J Miró-like paintings' or 'K Malewicz-like' paintings depending on atom nonidentity), see figures 1–9.

The rest of our paper is organized as follows: in section 2, we introduce the model Hamiltonian, then in section 3, we reduce the initial general Hamiltonian for vector bosons to the effective Hamiltonian appearing to be anisotropic spin-pseudospin model of the Kugel–Khomskii type [39]; in section 4, we investigate different possible configurations in spin and pseudospin spaces and find their energy; in section 5, we address the ground state energy of the system and the quantum phase transitions. In particular, in section 5, we illustrate the evolution of phase diagrams with the degree of atomic nonidentity, which looks like the transformation from the Joan Miró style artistic image to that of Kazimir Malewicz. Finally in the appendix, we present the analysis of several special limiting cases of the model Hamiltonian that relate our model system to some well-known results.

2. Hamiltonian for two species of vector bosons

We consider two types of boson atoms with $S = 1$ in the optical lattice with sites labeled by index i. The corresponding creation operators $c^{\dagger}_{i\alpha\sigma}$ where $\sigma = \{-1, 0, 1\}$ is the spin index and $\alpha = 1, 2$ labels the type of boson.

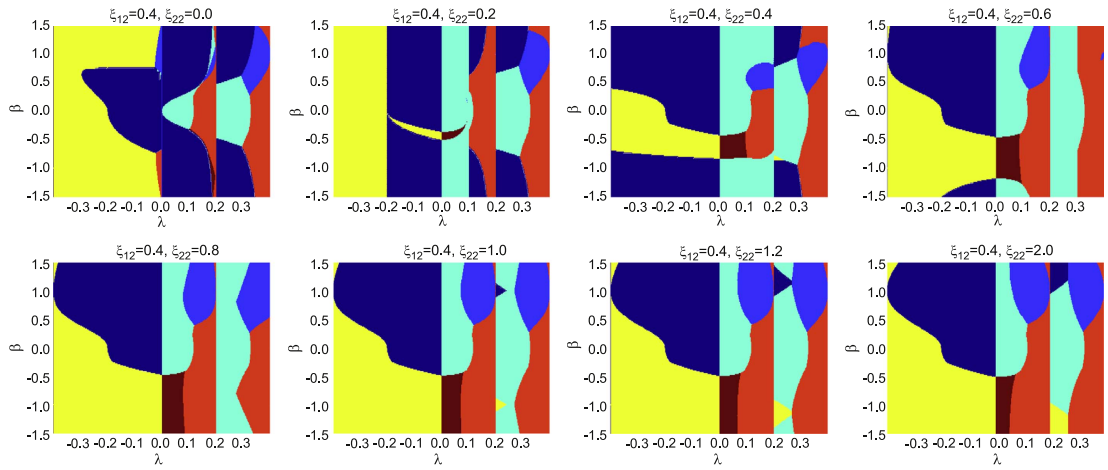

Figure 3. Phase diagrams for $\xi_{12} = U_{12}/U_{11} = 0.4$.

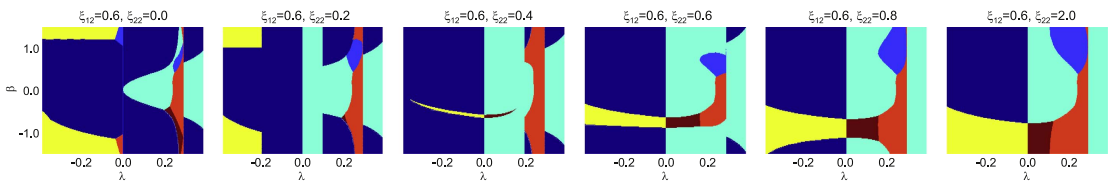

Figure 4. Phase diagrams for $\xi_{12} = U_{12}/U_{11} = 0.6$.

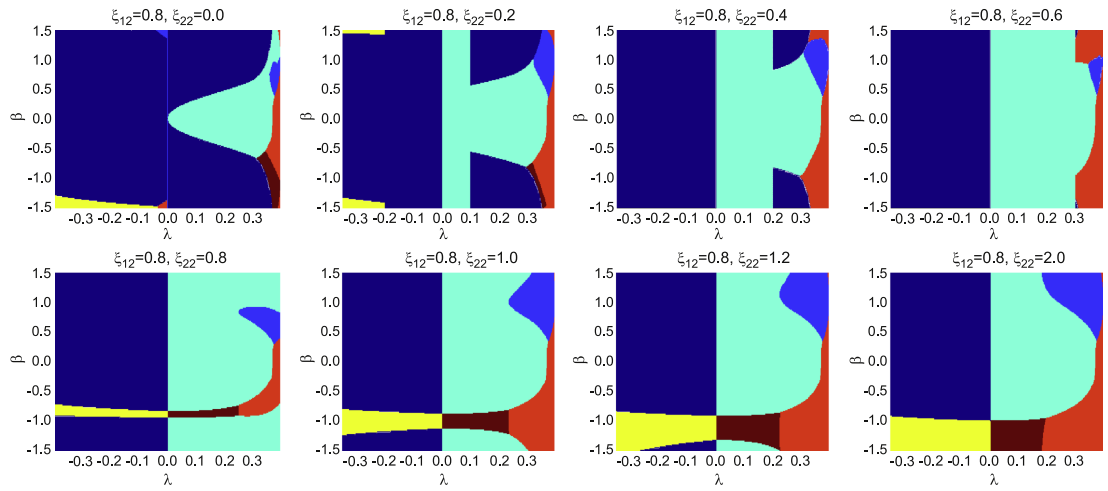

Figure 5. Phase diagrams for $\xi_{12} = U_{12}/U_{11} = 0.8$.

The Hamiltonian includes three terms:

$$H = H^{(U_0)} + H^{(U_s)} + H_t. \tag{1}$$

The interaction between bosons is given by two terms:

$$H^{(U_0)} = \sum_i U_{12} n_{i,1} n_{i,2} + \frac{1}{2} \sum_{i,\alpha=1,2} U_{\alpha\alpha} n_{i,\alpha}(n_{i,\alpha} - 1). \tag{2}$$

These terms corresponds to the repulsion between boson atoms at the same site [36]. Here, U_{11}, U_{22}, and U_{12} are three interaction parameters and $n_{i\alpha} = \sum_\sigma c^\dagger_{i\alpha\sigma} c_{i\alpha\sigma}$. Now we assume that the interaction constants can strongly differ from each other, in contrast to the case considered in [31].

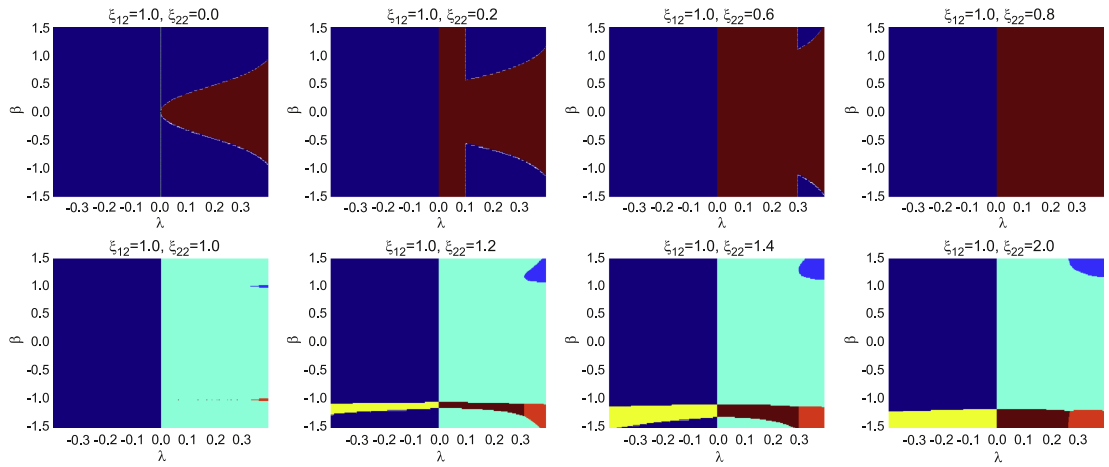

Figure 6. Phase diagrams for $\xi_{12} = U_{12}/U_{11} = 1.0$.

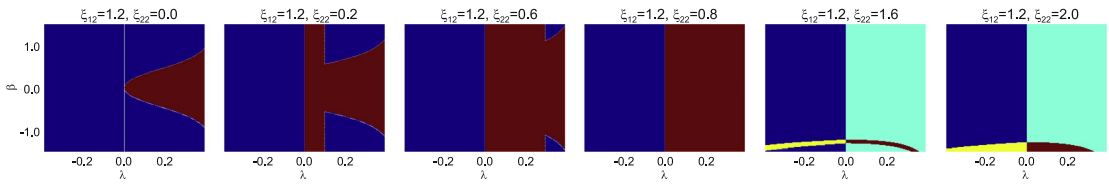

Figure 7. Phase diagrams for $\xi_{12} = U_{12}/U_{11} = 1.2$.

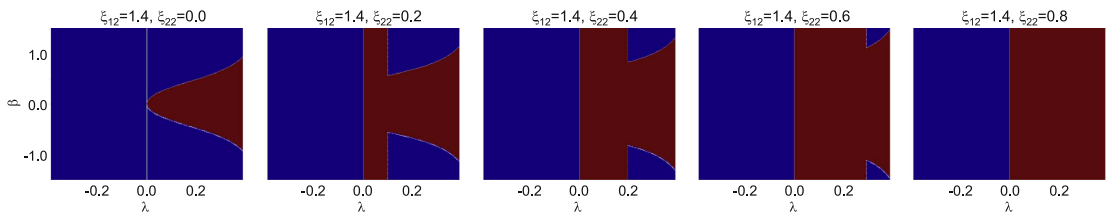

Figure 8. Phase diagrams for $\xi_{12} = U_{12}/U_{11} = 1.4$.

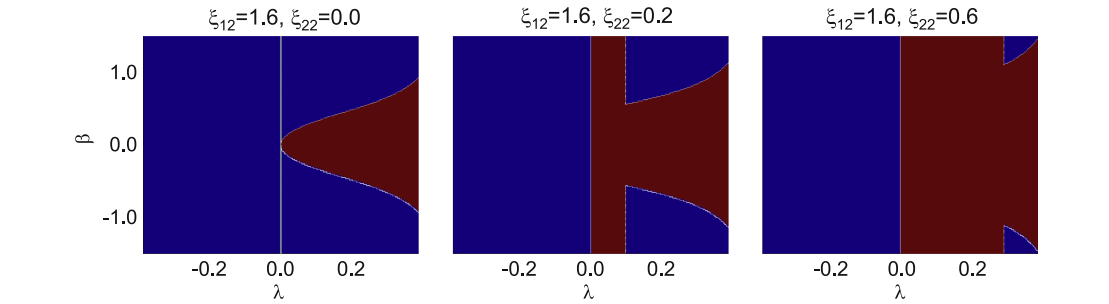

Figure 9. Phase diagrams for $\xi_{12} = U_{12}/U_{11} = 1.6$.

The spin-dependent interaction term is taken in the standard form [40, 41]:

$$H_i^{(U_s)} = U_s(\mathbf{S}_i^2 - 2n_i)/2, \tag{3}$$

where $n_i = n_{i,1} + n_{i,2}$ is the total number of bosons at site i.

The hopping term

$$H_t = \sum_{\langle i,j\rangle} h_t \equiv \sum_{\langle i,j\rangle} t_\alpha (c^\dagger_{i\alpha\sigma} c_{j\alpha\sigma} + c^\dagger_{j\alpha\sigma} c_{i\alpha\sigma}), \tag{4}$$

where $\langle i, j\rangle$ means the summation only over the nearest-neighbor sites and h_t is the hopping Hamiltonian for one link. As usual, the repeated indices imply summation.

3. Effective Hamiltonian

Below we focus on the Mott insulating state, where cold atoms are localized at the sites of optical lattice with the number of bosons at each site equal to unity. We remind that in such case, the hopping terms (4) can be treated as perturbation compared to the interaction part of the Hamiltonian, $H^{(U_0)} + H^{(U_s)}$. Application of the perturbation theory reduces the initial general Hamiltonian to a simpler effective Hamiltonian written solely in terms of the spin and pseudospin (p-spin) operators related to the lattice sites with atom filling equal to one. These spin-1 $\mathbf{S}_i$ and p-spin-1/2 $\boldsymbol{\mathcal{T}}_i$ operators are defined in a standard way [42]

$$S^a_i = c^\dagger_{i\alpha\sigma} s^a_{\sigma\sigma'} c_{i\alpha\sigma'}, \qquad \mathcal{T}^a_i = c^\dagger_{i\alpha\sigma} \tau^a_{\alpha\beta} c_{i\beta\sigma}, \tag{5}$$

where $a = x, y, z$.

Below we outline the algorithm of transforming the initial Hamiltonian to the effective one.

3.1. Basis states

In what follows, when we consider the link $\langle i, j\rangle$ between the nearest-neighbor sites, we focus on the basis of possible states for two bosons with spins $S_1 = 1$ and $S_2 = 1$ at neighboring sites $i = 1$ and $j = 2$. We are interested in the case with single occupation, i.e. when one boson of either type is located at each lattice site, $n_{i1} + n_{i2} = 1$. We can pass now to the basis of the eigenstates of the total spin squared $\mathbf{S}^2 = (\mathbf{S}_1 + \mathbf{S}_2)^2$ and its z-projection $S^z = S^z_1 + S^z_2$. We designate these states as $|SM\rangle$, $S = 0, 1, 2$ and $M = -\mathrm{S}, \ldots, S$. This basis can be written as follows

$$\Phi^{(f)}_{SM} = |\phi^{(f)}_S\rangle |SM\rangle, \tag{6}$$

where $f = 1, \ldots, 4$ enumerates the ways to distribute two types of bosons over two sites. The coordinate part $|\phi^{(f)}_S\rangle$ is given explicitly in [31].

Applying h_t, see equation (4), to the basis states (6), we obtain two kinds of intermediate (virtual) states. The first type will be realized for two *identical* bosons at one site (i or j), the second type is for two *nonidentical* bosons at one site. Intermediate energies depend on the spin and types of bosons. They are

$$\begin{aligned}
E^{aa}_{S=0} &= U_{11} - 2U_s, \quad & E^{aa}_{S=2} &= U_{11} + U_s,\\
E^{bb}_{S=0} &= U_{22} - 2U_s, \quad & E^{bb}_{S=2} &= U_{22} + U_s,\\
E^{ab}_{S=0} &= U_{12} - 2U_s, \quad & E^{ab}_{S=2} &= U_{12} + U_s,\\
E^{ab}_{S=1} &= U_{12} - U_s. &&
\end{aligned} \tag{7}$$

There are no intermediate states corresponding to the total spin $S = 1$ for two identical a- or b-bosons due to the symmetry of the total wave function [40].

The energy of the virtual states with the double site occupancy is much larger than the energy of the states with the single site occupancy we are focusing at. To find corrections to the energy of the single occupancy states related to the hoppings, we need the second-order terms of the perturbation theory. So, further it will be convenient to work with the operator

$$h = -h_{\mathrm{eff}} = h_t (1/H_0) h_t, \tag{8}$$

where $H_0 = H^{(U_0)} + H^{(U_s)}$. In the basis of states (6), the matrix of h can be presented in the following block form

$$h = \begin{pmatrix} B_{11} & 0 & 0 & 0\\ 0 & B_{22} & B_{23} & 0\\ 0 & B_{32} & B_{33} & 0\\ 0 & 0 & 0 & B_{44} \end{pmatrix}. \tag{9}$$

The matrix h here is in fact the block matrix, where each block is a 9×9 matrix. Blocks $B_{kl} = \langle \Phi^k_{S'M'} | h | \Phi^l_{SM} \rangle$, $k, l = 1, 2, 3, 4$ are diagonal matrices. Their explicit forms are the following

$$B_{11} = 4t_1^2 \begin{pmatrix} \frac{1}{E^{aa}_{S=0}} I_1 & & \\ & 0 \cdot I_3 & \\ & & \frac{1}{E^{aa}_{S=2}} I_5 \end{pmatrix}, \tag{10}$$

$$B_{44} = 4t_2^2 \begin{pmatrix} \frac{1}{E^{bb}_{S=0}} I_1 & & \\ & 0 \cdot I_3 & \\ & & \frac{1}{E^{bb}_{S=2}} I_5 \end{pmatrix}, \tag{11}$$

$$B_{22} = B_{33} = (t_1^2 + t_2^2) \begin{pmatrix} \frac{1}{E^{ab}_{S=0}} I_1 & & \\ & \frac{1}{E^{ab}_{S=1}} I_3 & \\ & & \frac{1}{E^{ab}_{S=2}} I_5 \end{pmatrix}, \tag{12}$$

$$B_{23} = B_{32} = 2t_1 t_2 \begin{pmatrix} \frac{1}{E^{ab}_{S=0}} I_1 & & \\ & \frac{1}{E^{ab}_{S=1}} I_3 & \\ & & \frac{1}{E^{ab}_{S=2}} I_5 \end{pmatrix}. \tag{13}$$

Here I_n, $n = 1, 3, 5$, are the identity $n \times n$ matrices. I_1 accounts for one state with $S = 0$, I_3 accounts for three states with $S = 1$, and I_5 accounts for five states with $S = 2$.

In what follows, we identify the single occupancy of site i with a- or b-boson by the pseudospin-1/2 states $|1\rangle_i = |+\rangle_i$ and $|2\rangle_i = |-\rangle_i$, respectively. It will be convenient to introduce explicitly two types of creation operators: $a^\dagger_{is}$ for bosons of type $\alpha = 1$ and $b^\dagger_{is}$ for bosons of type $\alpha = 2$.

For this purpose, we rewrite the pseudospin operator $\mathcal{T}^\gamma_i$ at sites i, see equation (5), in the form

$$\mathcal{T}^\gamma_i = a^\dagger_{is}\tau^\gamma_{11}a_{is} + a^\dagger_{is}\tau^\gamma_{12}b_{is} + b^\dagger_{is}\tau^\gamma_{21}a_{is} + b^\dagger_{is}\tau^\gamma_{22}b_{is}. \tag{14}$$

We can rewrite, as usual, the set of $\mathcal{T}^\gamma$ operators in the other equivalent form:

$$T^+_i = a^\dagger_{is}b_{is}, \quad T^-_i = b^\dagger_{is}a_{is}, \quad T^z_i = \frac{1}{2}(a^\dagger_{is}a_{is} - b^\dagger_{is}b_{is}). \tag{15}$$

To describe the occupancy of sites i and j, we introduce the basis of pseudospin states $|\alpha\beta\rangle = |\alpha\rangle_i|\beta\rangle_j$. Then, we find the correspondence between two-boson orbital states (6) and pseudospin states $|\alpha\beta\rangle$. For example, $|\phi^{(1)}_S\rangle \longrightarrow |{+}{+}\rangle$.

In what follows, we map the matrix h, equation (9), onto an effective spin-pseudospin operator in the space $|\alpha\rangle_i|\beta\rangle_j|SM\rangle$. This operator will be given in terms of spin $S = 1$ operators $\mathbf{S}_i$, $\mathbf{S}_j$ and pseudospin $T = 1/2$ operators $\mathbf{T}_i$, $\mathbf{T}_j$ and it has the same structure as matrix h, equation (9).

Next, we introduce the projection operator Q_S and P_T onto the combination of states $|SM\rangle$ and $|TM_T\rangle$ corresponding to the total spin $S = 0, 1, 2$ and pseudospin $T = 0, 1$ at the link $\langle i, j\rangle$. The projectors in the spin space $Q_S = \sum_{M=-S}^{S}|SM\rangle\langle SM|$ can be written as

$$\begin{aligned} Q_0 &= -\frac{1}{3} + \frac{1}{3}(\mathbf{S}_i \cdot \mathbf{S}_j)^2, \\ Q_1 &= 1 - \frac{1}{2}(\mathbf{S}_i \cdot \mathbf{S}_j) - \frac{1}{2}(\mathbf{S}_i \cdot \mathbf{S}_j)^2, \\ Q_2 &= \frac{1}{3} + \frac{1}{2}(\mathbf{S}_i \cdot \mathbf{S}_j) + \frac{1}{6}(\mathbf{S}_i \cdot \mathbf{S}_j)^2, \end{aligned} \tag{16}$$

where $Q_0 + Q_1 + Q_2 = 1$.

Similarly, in the pseudospin space the projectors onto the singlet $T = 0$ and triplet $T = 1$ states are

$$P_s = \frac{1}{4} - \mathbf{T}_i \cdot \mathbf{T}_j, \quad P_t = \frac{3}{4} + \mathbf{T}_i \cdot \mathbf{T}_j. \tag{17}$$

It is also convenient to introduce the following projectors in the pseudospin space

$$P^{11} = |{+}{+}\rangle\langle{+}{+}| = \left(\frac{1}{2} + T_i^z\right)\left(\frac{1}{2} + T_j^z\right),$$
$$P^{22} = |{+}{-}\rangle\langle{+}{-}| = \left(\frac{1}{2} + T_i^z\right)\left(\frac{1}{2} - T_j^z\right),$$
$$P^{33} = |{-}{+}\rangle\langle{-}{+}| = \left(\frac{1}{2} - T_i^z\right)\left(\frac{1}{2} + T_j^z\right),$$
$$P^{44} = |{-}{-}\rangle\langle{-}{-}| = \left(\frac{1}{2} - T_i^z\right)\left(\frac{1}{2} - T_j^z\right), \tag{18}$$

and

$$P^{32} = |{-}{+}\rangle\langle{+}{-}| = T_i^- T_j^+,$$
$$P^{23} = |{+}{-}\rangle\langle{-}{+}| = T_i^+ T_j^-. \tag{19}$$

In addition, we use below the following identities:

$$P^{11} + P^{44} = \frac{1}{2} + 2T_i^z T_j^z,$$
$$P^{22} + P^{33} = \frac{1}{2} - 2T_i^z T_j^z,$$
$$P^{32} + P^{23} = 2\mathbf{T}_i \cdot \mathbf{T}_j - 2T_i^z T_j^z. \tag{20}$$

With the help of projectors (16)–(19) and identities (20), we rewrite the block matrix h in terms of spin and pseudospin operators as follows

$$h = 4t_1^2\, P^{11}\left[\frac{Q_0}{E_0^{aa}} + \frac{Q_2}{E_2^{aa}}\right] + 4t_2^2\, P^{44}\left[\frac{Q_0}{E_0^{bb}} + \frac{Q_2}{E_2^{bb}}\right] + (t_1^2 + t_2^2)[P^{22} + P^{33}]\left[\frac{Q_0}{E_0^{ab}} + \frac{Q_1}{E_1^{ab}} + \frac{Q_2}{E_2^{ab}}\right]$$
$$+ 2t_1 t_2 [P^{23} + P^{32}]\left[\frac{Q_0}{E_0^{ab}} + \frac{Q_1}{E_1^{ab}} + \frac{Q_2}{E_2^{ab}}\right]. \tag{21}$$

Substituting the explicit form of pseudospin projectors, we can rewrite h in the form

$$h = \left\{\frac{t_1^2}{E_0^{aa}} + \frac{t_2^2}{E_0^{bb}} + 2\left(\frac{t_1^2}{E_0^{aa}} - \frac{t_2^2}{E_0^{bb}}\right)(T_i^z + T_j^z) + 4\left(\frac{t_1^2}{E_0^{aa}} + \frac{t_2^2}{E_0^{bb}}\right)T_i^z T_j^z\right\}Q_0$$
$$+ \left\{\frac{t_1^2}{E_2^{aa}} + \frac{t_2^2}{E_2^{bb}} + 2\left(\frac{t_1^2}{E_2^{aa}} - \frac{t_2^2}{E_2^{bb}}\right)(T_i^z + T_j^z) + 4\left(\frac{t_1^2}{E_2^{aa}} + \frac{t_2^2}{E_2^{bb}}\right)T_i^z T_j^z\right\}Q_2$$
$$+ \left\{\frac{1}{2}(t_1^2 + t_2^2) - 2(t_1 + t_2)^2 T_i^z T_j^z + 4t_1 t_2\, \mathbf{T}_i \cdot \mathbf{T}_j\right\}\left[\frac{Q_0}{E_0^{ab}} + \frac{Q_1}{E_1^{ab}} + \frac{Q_2}{E_2^{ab}}\right]. \tag{22}$$

Finally, the effective Hamiltonian is written as the sum of h operators (22) over all $\langle i, j\rangle$ links

$$H_{\text{eff}} = -\sum_{\langle i,j\rangle} h. \tag{23}$$

This is the most general form of the effective Hamiltonian involving different Hubbard interaction parameters, different hopping amplitudes, and spin-dependent interaction. In the appendix, we show that in a number of limiting cases, this Hamiltonian can be simplified to some well-known forms.

4. Energy of the ground state

To proceed with the calculation of the ground state energy, we rewrite the 'kernel' h of effective Hamiltonian (23) as follows

$$h = \frac{2t_1^2}{U_{11}}\left(R_0 Q_0 + R_2 Q_2 + R_1\left[\frac{Q_0}{E_0^{ab}} + \frac{Q_1}{E_1^{ab}} + \frac{Q_2}{E_2^{ab}}\right]\right), \tag{24}$$

where the coefficients R_0, R_1 and R_2 are

$$R_0 = \left[\frac{1}{2}\left(\frac{1}{E_0^{aa}} + \frac{\beta^2}{E_0^{bb}}\right) + \left(\frac{1}{E_0^{aa}} - \frac{\beta^2}{E_0^{bb}}\right)(T_i^z + T_j^z) + 2\left(\frac{1}{E_0^{aa}} + \frac{\beta^2}{E_0^{bb}}\right)(T_i^z T_j^z)\right], \tag{25}$$

$$R_1 = \left[\frac{1}{4}(1+\beta^2) - (1+\beta)^2(T_i^z T_j^z) + 2\beta(\mathbf{T}_i \cdot \mathbf{T}_j)\right], \tag{26}$$

$$R_2 = \left[\frac{1}{2}\left(\frac{1}{E_2^{aa}} + \frac{\beta^2}{E_2^{bb}}\right) + \left(\frac{1}{E_2^{aa}} - \frac{\beta^2}{E_2^{bb}}\right)(T_i^z + T_j^z) + 2\left(\frac{1}{E_2^{aa}} + \frac{\beta^2}{E_2^{bb}}\right)(T_i^z T_j^z)\right]. \tag{27}$$

Here, we introduce the dimensionless parameter $\beta = t_2/t_1$ that characterizes the difference of the tunnel amplitudes for different boson species.

The energy E of the ground state can be formally written as the average of the effective Hamiltonian over the ground state wave function (we will find it later using the variational approach)

$$E = -\frac{\nu}{2}\langle h\rangle, \tag{28}$$

where $\nu = 2D$ is the number of nearest neighbors for the D-dimensional cubic lattice.

Within the mean-field approximation, we can neglect any correlations between spin and p-spin degrees of freedom. Then, for example, $\langle R_0 Q_0\rangle \rightarrow \langle R_0\rangle\langle Q_0\rangle$, and

$$\langle h\rangle = E_u\left(\langle R_0\rangle\langle Q_0\rangle + \langle R_2\rangle\langle Q_2\rangle + \langle R_1\rangle\left[\frac{\langle Q_0\rangle}{E_0^{ab}} + \frac{\langle Q_1\rangle}{E_1^{ab}} + \frac{\langle Q_2\rangle}{E_2^{ab}}\right]\right), \tag{29}$$

where $E_u = \frac{2t_1^2}{U_{11}}$.

We take the trial wave function in the p-spin space as the 'mixed orbital state' on two-sublattices A and B

$$|\chi\rangle_i = \cos\theta|+\rangle_i + \sin\theta|-\rangle_i, \quad i \in A, \tag{30}$$

$$|\chi\rangle_j = \cos\theta|+\rangle_j + \eta\sin\theta|-\rangle_j, \quad j \in B, \quad \eta = \pm 1. \tag{31}$$

For $\theta = 0$, it defines the p-spin ferromagnetic (FM) state

$$|\uparrow_i \uparrow_j \uparrow_i \uparrow_j \ldots\rangle. \tag{32}$$

For $\theta = \frac{\pi}{2}$, it defines also the p-spin FM state

$$|\downarrow_i (-\downarrow_j)\downarrow_i (-\downarrow_j)\ldots\rangle. \tag{33}$$

The FM and AFM p-spin states will occur at $\theta = \frac{\pi}{4}$ for $\eta = +1$ and $\eta = -1$, respectively. These states are polarized in x direction:

$$\frac{1}{\sqrt{2}}(|\uparrow\rangle + |\downarrow\rangle)_i, \tag{34}$$

$$\frac{1}{\sqrt{2}}(|\uparrow\rangle + \eta|\downarrow\rangle)_j. \tag{35}$$

For other angles θ, the mixed orbital state is a some intermediate state between the FM and AFM ones. That is why, it is more correctly to refer to this mixed orbital state as the mixed orbital state with $\eta = +1$, or $\eta = -1$ rather than the FM and AFM states.

Now, we find averages over the trial mixed orbital state of the p-spin operators entering R_i, $i = 0, 1, 2$

$$\langle T_i^z + T_j^z\rangle = \begin{cases} \cos 2\theta, & \eta = +1, \\ 0, & \eta = -1, \end{cases} \tag{36}$$

$$\langle T_i^z T_j^z\rangle = \begin{cases} \frac{1}{4}\cos^2 2\theta, & \eta = +1, \\ -\frac{1}{4}\cos^2 2\theta, & \eta = -1, \end{cases} \tag{37}$$

$$\langle \mathbf{T}_i \mathbf{T}_j\rangle = \begin{cases} \frac{1}{4}, & \eta = +1, \\ -\frac{1}{4}, & \eta = -1. \end{cases} \tag{38}$$

Later on, we will minimize the energy E with respect to the angle θ.

In contrast to the p-spin space, the effective Hamiltonian in the spin space is isotropic. So, we do not expect any exotic states there. Hence, we take for trial wave functions in the spin space the usual FM, AFM, and nematic (NEM) states. It should be noted that NEM naturally appears for spin-1 isotropic Heisenberg Hamiltonian, it has zero average site spin, and it is discussed in detail in [40].

Then, the coefficients for projectors in the spin space are

$$\langle Q_0\rangle = \begin{cases} 0, & \text{FM},\\ \frac{1}{3}, & \text{AFM},\\ \frac{1}{3}, & \text{NEM}, \end{cases} \qquad \langle Q_1\rangle = \begin{cases} 0, & \text{FM},\\ \frac{1}{2}, & \text{AFM},\\ 0, & \text{NEM}, \end{cases}$$
$$\langle Q_2\rangle = \begin{cases} 1, & \text{FM},\\ \frac{1}{6}, & \text{AFM},\\ \frac{2}{3}, & \text{NEM}. \end{cases} \tag{39}$$

Finally, we have found all the averages and correlation functions entering equation (28) for the energy. We minimize numerically the energy $E(\theta, \eta)$, find the ground stats at different values of the parameters, and draw the corresponding phase diagrams.

5. Results and discussion

5.1. General properties of the phase diagrams

We address here the ground state of the system and possible quantum phase transitions. Performing the energy minimization, we find the phase diagrams for different ranges of the parameters. The key parameters are $\beta = t_2/t_1, \lambda = U_s/U_{11}, \xi_{12} = U_{12}/U_{11}$, and $\xi_{22} = U_{22}/U_{11}$. All these parameters (except λ responsible for spin channel interaction) are related to the difference between the types of bosons.

There are six different phases: three phases have the FM pseudospin arrangement, while three others correspond to the AFM pseudospin state. Evolution of these phases is illustrated in figures 1–9; figure 1 is supplemented by the colorbar, where the correspondence between colors and phases is shown. Points at the colorbar correspond to the following orders in spin and pseudospin systems:

$$\begin{aligned} 1 &\to E^{\text{p-spin FM}}_{\text{FM}},\\ 2 &\to E^{\text{p-spin FM}}_{\text{AFM}},\\ 3 &\to E^{\text{p-spin FM}}_{\text{NEM}},\\ 4 &\to E^{\text{p-spin AFM}}_{\text{FM}},\\ 5 &\to E^{\text{p-spin AFM}}_{\text{AFM}},\\ 6 &\to E^{\text{p-spin AFM}}_{\text{NEM}}. \end{aligned} \tag{40}$$

Here, for example, color '1' corresponds to FM spin and pseudospin orders.

In figures 1–9, we demonstrate the evolution of the phase diagrams within the wide range of parameters $\beta = t_2/t_1, \lambda = U_s/U_{11}, \xi_{12} = U_{12}/U_{11}$ and $\xi_{22} = U_{22}/U_{11}$. The most interesting phase transition is that accompanied by the change of atom distribution over the optical lattice: p-spin FM $\leftrightarrow$ p-spin AFM. Note that the cold colors correspond to FM p-spin, while the warm ones—to p-spin AFM. So the transitions with p-spin change can be found in the phase diagram at the lines, where cold colors change to warm ones.

Evolution of the phase diagrams for $\xi_{12} = U_{12}/U_{11} = 0$ with $\xi_{22} = U_{22}/U_{11}$ on (λ, β)-plane is shown in figure 1. In this case, there is no Coulomb interaction between different boson species. We see that there is always quantum phase transition at the line $\lambda = 0$. This is true not only for figure 1, but also for all phase diagrams in figures 1–9. This phase transition is driven by the sign change of spin channel interaction U_s. This transition has been recently revealed in [31] for nearly identical vector bosons. Here, we show that this transition is quite robust with respect to the evolution of the degree of nonidentity.

One can also see in figure 1, that the 'left color' is always blue. It corresponds to FM spin ordering (with FM p-spin ordering). This situation is intuitively obvious: since the 'left' phase is determined by large negative λ—the interaction in the spin channel. In all the next figures, the 'left color' also corresponds to the FM spin ordering, sometimes with the AFM p-spin ordering (yellow).

Looking through the complete set of phase diagrams, one can notice the absence of exact symmetry with the respect to reflections $\lambda \to -\lambda$ and $\beta \to -\beta$, though some traces are detectable. The β-symmetry is restored, when $\xi_{12} \gg \xi_{22}$.

Let us mention that the intuitive speculations useful, for example, in the case of simple Heisenberg model, can be misleading here, because the effective Hamiltonian is rather nontrivial.

We also underline the evolution of the artistic image of the phase diagrams. Namely, at small ξ_{12} their style resembles the J Miró paintings, while at large ξ_{12}—those of K Malewicz.

5.2. Phase diagrams: specific features

Figures 1 and 2 are the most multicolored—there are quantum phase transitions nearly between all the possible phases. These pictures correspond to the low or moderate interspecies Coulomb interaction U_{12} as compared to the single-species one. This feature can be attributed to small or moderate difference in the parameters characterizing their nonidentity. One can also notice that there are many reentrant phase transitions in figures 1–9, especially for moderate ξ_{12}.

When ξ_{22} becomes sufficiently large, then the NEM spin phase prevails. The ξ_{22}-threshold for this behavior is the smallest at large ξ_{12}, as can be seen in figures 1–9.

6. Conclusions

To conclude, we have investigated the evolution of the quantum state of vector two species bosons in optical lattices with the 'degree of atomic nonidentity' that drives the cascade of quantum phase transitions. Surprisingly, this quite simple model exhibits rather rich and complicated manifold of quantum phase transitions between six different phases when interaction parameters of the model change in rather limited subspace. In fact, one can say that the system is 'unstable' with the respect to small variation of parameters.

Technically, we have reduced the initial general Hamiltonian for vector bosons, using the Mott insulating state natural small parameters, to the anisotropic spin-pseudospin model of the Kugel–Khomskii type that served as the effective Hamiltonian. This procedure gave a chance for analytical progress in investigations of the system ground state. The variational approach have been used to uncover the phase diagram of the system in hand. Finally, we have investigated also limiting cases of the effective Hamiltonian and demonstrated the relation of our rather complicated Hamiltonian to the well-known results. There are further perspectives to find new results in the two species fermion systems in optical lattices and hybrid boson-fermion ones looking at the 'degree of atomic nonidentity' as the driving parameter.

Acknowledgments

AM and AB are grateful to Wu-Ming Liu for interest to this work and hospitality in Beijing National Laboratory for Condensed Matter Physics. NC is grateful to A Pekovic for stimulating discussions at the initial stage of this work, to Laboratoire de Physique Théorique, Toulouse, where this work has been initiated, for the hospitality, and to CNRS.

This work was supported by the Russian Foundation for Basic Research (projects Nos. 16-02-00295, 16-02-00304, 17-52-53014, and 17-02-00323). We also express our gratitude to Government of the Russian Federation (project No. 05.Y09.21.0018) for support of the preparation of this paper revised version and the Computational Centers of Russian Academy of Sciences and National Research Center 'Kurchatov Institute' for providing the access to URAL, JSCC, and HPC facilities.

Appendix. Special cases of Hamiltonian (22)–(23)

We remind that $H_{\rm eff} = -\sum_{\langle i,j\rangle} h$.

A.1. Equal Hubbard interaction parameters

Now, we take a look at more special cases. First we consider the case with equal Hubbard interaction parameters

$$U_{12} = U_{11} = U_{22} = U_0. \tag{A.1}$$

Then

$$E_S^{ab} = E_S^{aa} = E_S^{bb} = E_S, \qquad S = 0,\ 1,\ 2, \tag{A.2}$$

and as follows from equation (22), the effective matrix h reduces to the following form:

$$\begin{aligned} h = {} & \frac{Q_0}{E_0}\left\{\frac{3}{2}(t_1^2 + t_2^2) + 2(t_1^2 - t_2^2)(T_i^z + T_j^z) + 2(t_1 - t_2)^2\, T_i^z T_j^z + 4t_1 t_2\, \mathbf{T}_i \cdot \mathbf{T}_j\right\} \\ & + \frac{Q_2}{E_2}\left\{\frac{3}{2}(t_1^2 + t_2^2) + 2(t_1^2 - t_2^2)(T_i^z + T_j^z) + 2(t_1 - t_2)^2\, T_i^z T_j^z + 4t_1 t_2\, \mathbf{T}_i \cdot \mathbf{T}_j\right\} \\ & + \frac{Q_1}{E_1}\left\{\frac{1}{2}(t_1^2 + t_2^2) - 2(t_1 + t_2)^2\, T_i^z T_j^z + 4t_1 t_2\, \mathbf{T}_i \cdot \mathbf{T}_j\right\}. \end{aligned} \tag{A.3}$$

A.2. Equal Hubbard interaction parameters and equal hopping amplitudes

The effective matrix h can be simplified further if one considers equal hopping amplitudes, $t_1 = t_2 = t$. For this case, as it can be seen from equation (A.3), matrix h reduces to

$$h = \frac{Q_0}{E_0}\{3t^2 + 4t^2\,\mathbf{T}_i \cdot \mathbf{T}_j\} + \frac{Q_2}{E_2}\{3t^2 + 4t^2\,\mathbf{T}_i \cdot \mathbf{T}_j\} + \frac{Q_1}{E_1}\{t^2 - 8t^2\,T_i^z T_j^z + 4t^2\,\mathbf{T}_i \cdot \mathbf{T}_j\}. \tag{A.4}$$

The last expression can be simplified if we take into account that

$$t^2 - 8t^2\,T_i^z T_j^z + 4t^2\,\mathbf{T}_i \cdot \mathbf{T}_j = 4t^2\,P_{t0}, \tag{A.5}$$

where $P_{t0} = P_t - (P^{11} + P^{44}) = [1/4 - 2T_i^z T_j^z + \mathbf{T}_i \cdot \mathbf{T}_j]$ is the projector onto the pseudospin state $|T = 1,\ M_T = 0\rangle$, when the matrix h can be reduced to the form

$$h = 4t^2\left\{\frac{Q_0}{E_0}P_t + \frac{Q_2}{E_2}P_t + \frac{Q_1}{E_1}P_{t0}\right\}. \tag{A.6}$$

Note that due to the presence of the projector P_{t0}, the states with spin $S = 1$ will be automatically symmetric in the orbital space, while the antisymmetric combination of orbital states is automatically excluded from the effective Hamiltonian.

Next, we rewrite the Hamiltonian h in terms of the spin operators. We use the relation

$$\begin{aligned} -4t^2\left(\frac{Q_0}{E_0} + \frac{Q_2}{E_2}\right) &= \left\{\frac{-4t^2}{3}\left(\frac{1}{E_2} - \frac{1}{E_0}\right) + \frac{-4t^2}{2E_2}\,\mathbf{S}_i \cdot \mathbf{S}_j + \frac{-4t^2}{3}\left(\frac{1}{E_0} + \frac{1}{2E_2}\right)(\mathbf{S}_i \cdot \mathbf{S}_j)^2\right\} \\ &= \epsilon + J\,\mathbf{S}_i \cdot \mathbf{S}_j + K\,(\mathbf{S}_i \cdot \mathbf{S}_j)^2, \end{aligned} \tag{A.7}$$

where

$$J = \frac{-2t^2}{E_2}, \quad K = \frac{-4t^2}{3}\left(\frac{1}{E_0} + \frac{1}{2E_2}\right), \tag{A.8}$$

$$\epsilon = \frac{-4t^2}{3}\left(\frac{1}{E_2} - \frac{1}{E_0}\right) = J - K. \tag{A.9}$$

Parameters J, K, and ϵ can be expressed explicitly via the initial interaction constants U_0 and U_s as follows

$$J = \frac{-2t^2}{U_0 + U_s}, \quad K = \frac{-2t^2 U_0}{(U_0 + U_s)(U_0 - 2U_s)}, \tag{A.10}$$

$$\epsilon = \frac{4t^2 U_s}{(U_0 + U_s)(U_0 - 2U_s)}. \tag{A.11}$$

Now, the Hamiltonian takes the form

$$H_{\text{eff}} = \sum_{\langle i,j\rangle}\left\{[\epsilon + J\,\mathbf{S}_i \cdot \mathbf{S}_j + K\,(\mathbf{S}_i \cdot \mathbf{S}_j)^2]P_t + \left(\frac{-4t^2}{E_1}\right)Q_1 P_{t0}\right\}. \tag{A.12}$$

Finally, the relation $P_t = P_{t0} + P^{11} + P^{44}$ and the definition of Q_1 (16) allows us to reduce the Hamiltonian to the form used in [31],

$$H_{\text{eff}} = \sum_{\langle i,j\rangle}\{[\epsilon + J\,\mathbf{S}_i \cdot \mathbf{S}_j + K\,(\mathbf{S}_i \cdot \mathbf{S}_j)^2](P^{11} + P^{44}) + [\epsilon' + J'\,\mathbf{S}_i \cdot \mathbf{S}_j + K'\,(\mathbf{S}_i \cdot \mathbf{S}_j)^2]\,P_{t0}\}, \tag{A.13}$$

where we introduced

$$J' = 2t^2\left(\frac{1}{E_1} - \frac{1}{E_2}\right), \tag{A.14}$$

$$K' = \frac{-2t^2}{3}\left(\frac{2}{E_0} + \frac{1}{E_2} - \frac{3}{E_1}\right), \tag{A.15}$$

$$\epsilon' = \frac{-4t^2}{3}\left(\frac{1}{E_2} - \frac{1}{E_0} + \frac{3}{E_1}\right). \tag{A.16}$$

A.2.1. One type of bosons. For the case of only one type of bosons, Hamiltonian (A.13) is equivalent to that of [43]. For single type of bosons, the pseudospin operators become c-numbers: $T_i^z = \pm 1/2$, $\mathbf{T}_i \cdot \mathbf{T}_j$ should be replaced by $T_i^z T_j^z = 1/4$, and projectors $P^{11} + P^{44} = 1$, $P_{t0} = 0$. Then equation (A.13) is reduced to the Hamiltonian considered in [43]

$$H_{\rm eff} = \sum_{\langle i,j\rangle}\{\epsilon + J\ \mathbf{S}_i\cdot\mathbf{S}_j + K\ (\mathbf{S}_i\cdot\mathbf{S}_j)^2\}. \tag{A.17}$$

A.2.2. No spin-dependent interaction. If there is no spin-dependent interaction, i.e. $U_s = 0$, then $E_0 = E_2 = E_1$ and $J = K = -2t^2/U_0, \epsilon = 0, J' = K' = 0$, and $\epsilon' = -4t^2/U_0 = 2J$. The effective Hamiltonian, equation (A.13), is reduced to

$$H_{\rm eff} = J\sum_{\langle i,j\rangle}\{2P_{t0} + (\mathbf{S}_i\cdot\mathbf{S}_j + (\mathbf{S}_i\cdot\mathbf{S}_j)^2)(P^{11} + P^{44})\}. \tag{A.18}$$

And at last, if in this case, there is only one type of bosons, then $P_{t0} = 0$, $P^{11} + P^{44} = 1$, and the effective Hamiltonian describing effective interaction between identical bosons has the FM character ($J < 0$)

$$H_{\rm eff} = J\sum_{\langle i,j\rangle}\{\mathbf{S}_i\cdot\mathbf{S}_j + (\mathbf{S}_i\cdot\mathbf{S}_j)^2\}, \quad J = \frac{-2t^2}{U_0}. \tag{A.19}$$

The systems with identical bosons with odd and even number bosons per site were discussed in [40, 41].

ORCID iDs

N M Chtchelkatchev https://orcid.org/0000-0002-7242-1483
A V Mikheyenkov https://orcid.org/0000-0003-4030-5426

References

[1] Greiner M, Mandel O, Esslinger T, Hänsch T W and Bloch I 2002 Quantum phase transition from a superfluid to a Mott insulator in a gas of ultracold atoms *Nature* **415** 39–44
[2] Köhl M, Moritz H, Stöferle T, Günter K and Esslinger T 2005 Fermionic atoms in a three dimensional optical lattice: observing Fermi surfaces, dynamics, and interactions *Phys. Rev. Lett.* **94** 080403
[3] Ji A-C, Liu W-M, Song J L and Zhou F 2008 Dynamical creation of fractionalized vortices and vortex lattices *Phys. Rev. Lett.* **101** 010402
[4] Qi R, Yu X-L, Li Z B and Liu W-M 2009 Non-Abelian Josephson effect between two $f = 2$ spinor Bose–Einstein condensates in double optical traps *Phys. Rev. Lett.* **102** 185301
[5] Kawaguchi Y and Ueda M 2012 Spinor Bose–Einstein condensates *Phys. Rep.* **253** 253–381
[6] Chen Y-H, Tao H-S, Yao D-X and Liu W-M 2012 Kondo metal and ferrimagnetic insulator on the triangular kagome lattice *Phys. Rev. Lett.* **108** 246402
[7] Hauke P, Cucchietti F M, Tagliacozzo L, Deutsch I and Lewenstein M 2012 Can one trust quantum simulators? *Rep. Prog. Phys.* **75** 082401
[8] Baier S, Mark M J, Petter D, Aikawa K, Chomaz L, Cai Z, Baranov M, Zoller P and Ferlaino F 2016 Extended Bose–Hubbard models with ultracold magnetic atoms *Science* **352** 201–5
[9] Bermudez A, Tagliacozzo L, Sierra G and Richerme P 2017 Long-range Heisenberg models in quasiperiodically driven crystals of trapped ions *Phys. Rev.* B **95** 024431
[10] Mazurenko A, Chiu C S, Ji G, Parsons M F, Kanász-Nagy M, Schmidt R, Grusdt F, Demler E, Greif D and Greiner M 2017 A cold-atom Fermi–Hubbard antiferromagnet *Nature* **545** 462–6
[11] Decamp J, Jnemann J, Albert M, Rizzi M, Minguzzi A and Vignolo P 2017 Strongly correlated one-dimensional Bose–Fermi quantum mixtures: symmetry and correlations *New J. Phys.* **19** 125001
[12] Lvque C and Madsen L B 2017 Time-dependent restricted-active-space self-consistent-field theory for bosonic many-body systems *New J. Phys.* **19** 043007
[13] Duncan C W, Bellotti F F, Öhberg P, Zinner N T and Valiente M 2017 Mobile spin impurity in an optical lattice *New J. Phys.* **19** 075001
[14] Sun F, Ye J and Liu W-M 2017 Fermionic Hubbard model with Rashba or Dresselhaus spin–orbit coupling *New J. Phys.* **19** 063025
[15] Meacher D R 1998 Optical lattices-crystalline structures bound by light *Contemp. Phys.* **39** 329–50
[16] Jaksch D, Bruder C, Cirac J I, Gardiner C W and Zoller P 1998 Cold bosonic atoms in optical lattices *Phys. Rev. Lett.* **81** 3108–11
[17] Grimm R, Weidemuller M and Ovchinnikov Y B 2000 Optical dipole traps for neutral atoms *Adv. At., Mol., Opt. Phys.* **42** 95–170
[18] Corboz P, Lajkó M, Läuchli A M, Penc K and Mila F 2012 Spin-orbital quantum liquid on the honeycomb lattice *Phys. Rev.* X **2** 041013
[19] Schaetz T, Monroe C R and Esslinger T 2013 Focus on quantum simulation *New J. Phys.* **15** 085009
[20] Gonzlez-Cuadra D, Zohar E and Cirac J I 2017 Quantum simulation of the Abelian–Higgs lattice gauge theory with ultracold atoms *New J. Phys.* **19** 063038
[21] Min J, Söyler Ş G, Rotondo P and Lesanovsky I 2017 Effective spin physics in two-dimensional cavity QED arrays *New J. Phys.* **19** 063033
[22] Kuklov A B and Svistunov B V 2003 Counterflow superfluidity of two-species ultracold atoms in a commensurate optical lattice *Phys. Rev. Lett.* **90** 100401
[23] Paredes B, Widera A, Murg V, Mandel O, Fölling S, Cirac I, Shlyapnikov G V, Hänsch T W and Bloch I 2004 Tonks–Girardeau gas of ultracold atoms in an optical lattice *Nature* **429** 277
[24] Isacsson A, Cha M-C, Sengupta K and Girvin S M 2005 Superfluid-insulator transitions of two-species bosons in an optical lattice *Phys. Rev.* B **72** 184507
[25] Mishra T, Pai R V and Das B P 2007 Phase separation in a two-species Bose mixture *Phys. Rev.* A **76** 013604
[26] Hubener A, Snoek M and Hofstetter W 2009 Magnetic phases of two-component ultracold bosons in an optical lattice *Phys. Rev.* B **80** 245109
[27] Takayoshi S, Sato M and Furukawa S 2010 Spontaneous population imbalance in two-component Bose and Fermi gases *Phys. Rev.* A **81** 053606

[28] Chung C-M, Fang S and Chen P 2012 Quantum and thermal transitions out of the pair-supersolid phase of two-species bosons on a square lattice *Phys. Rev.* B **85** 214513
[29] Belemuk A M, Chtchelkatchev N M and Mikheyenkov A V 2014 Effective orbital ordering in multiwell optical lattices with fermionic atoms *Phys. Rev.* A **90** 023625
[30] Abanin D A, De Roeck W and Huveneers F 2015 Exponentially slow heating in periodically driven many-body systems *Phys. Rev. Lett.* **115** 256803
[31] Belemuk A M, Chtchelkatchev N M, Mikheyenkov A V and Kugel K I 2017 Magnetic phase diagram and quantum phase transitions in a two-species boson model *Phys. Rev.* B **96** 094435
[32] Potirniche I-D, Potter A C, Schleier-Smith M, Vishwanath A and Yao N Y 2017 Floquet symmetry-protected topological phases in cold-atom systems *Phys. Rev. Lett.* **119** 123601
[33] Penna V and Richaud A 2017 Two-species boson mixture on a ring: a group-theoretic approach to the quantum dynamics of low-energy excitations *Phys. Rev.* A **96** 053631
[34] Hu S, Wang T, Pelster A, Eggert S and Zhang X 2018 Periodically modulated interaction of two species bosons on the optical lattice *Bull. Am. Phys. Soc.* https://meetings.aps.org/Meeting/MAR18/Session/P26.5
[35] Georgescu I M, Ashhab S and Nori F 2014 Quantum simulation *Rev. Mod. Phys.* **86** 153–85
[36] Dutta O, Gajda M, Hauke P, Lewenstein M, Luhmann D-S, Malomed B A, Sowinski T and Zakrzewski J 2015 Non-standard Hubbard models in optical lattices: a review *Rep. Prog. Phys.* **78** 066001
[37] Gross C and Bloch I 2017 Quantum simulations with ultracold atoms in optical lattices *Science* **357** 995–1001
[38] Krutitsky K V 2016 Ultracold bosons with short-range interaction in regular optical lattices *Phys. Rep.* **607** (Suppl. C) 1–101
[39] Kugel K I and Khomskii D I 1982 The Jahn–Teller effect and magnetism: transition metal compounds *Sov. Phys.—Usp.* **25** 231–56
[40] Imambekov A, Lukin M and Demler E 2003 Spin-exchange interactions of spin-one bosons in optical lattices: singlet, nematic, and dimerized phases *Phys. Rev.* A **68** 063602
[41] Tsuchiya S, Kurihara S and Kimura T 2004 Superfluid–Mott insulator transition of spin-1 bosons in an optical lattice *Phys. Rev.* A **70** 043628
[42] Yamashita Y, Shibata N and Ueda K 1998 *Su*(4) spin–orbit critical state in one dimension *Phys. Rev.* B **58** 9114–8
[43] Yip S K 2003 Dimer state of spin-1 bosons in an optical lattice *Phys. Rev. Lett.* **90** 250402